Available online at www.sciencedirect.com
ScienceDirect
Powder Technology 181 (2008) 307–320
POWDER TECHNOLOGY
www.elsevier.com/locate/powtec

Agglomeration in fluidised bed gasification of biomass

L.E. Fryda *, K.D. Panopoulos, E. Kakaras

Laboratory of Steam Boilers and Thermal Plants, School of Mechanical Engineering, Thermal Engineering Section, National Technical University of Athens, 9 Heroon Polytechniou Ave., Zografou 15780, Greece

Received 13 February 2006; received in revised form 17 February 2007; accepted 17 May 2007
Available online 29 May 2007

Abstract

Three promising biomass fuels for southern Mediterranean regions were tested for their agglomeration tendency in an atmospheric lab-scale fluidised bed (FB) gasifier using quartz and olivine as bed materials. The defluidisation temperatures of the energy crops Giant Reed (*Arundo donax* L.) and Sweet Sorghum bagasse were respectively approx. 790 °C and 810 °C, in both bed materials, while the agro industrial residue olive bagasse caused defluidisation of the quartz bed at 830 °C and olivine bed at >850 °C. Agglomerates from these tests were analysed with SEM/EDS. Coatings and necks between bed particles were formed due to ash derived potassium silicate melt. For the first two fuels cluster-type agglomerates around remains of char particles were observed. Thermodynamic equilibrium simulations of each chemical system were performed to cross examine the predicted ash melting temperatures and chemistry with experimental findings. Predictions of potassium liquid compounds, like $K_2O{\cdot}SiO_{2(l)}$ were verified by EDS analyses on the particle coatings. FB gasification of olive bagasse resisted defluidisation up to higher temperatures because of its lower potassium and higher calcium content, especially in the case of olivine bed. The latter experimental finding coincided with thermodynamic predictions.
© 2007 Elsevier B.V. All rights reserved.

Keywords: Fluidised bed; Agglomeration; Biomass; Gasification; SEM/EDS; FactSAGE™

1. Introduction

Biomass fuels such as agricultural or agro industrial residues together with energy crops are considered promising renewable energy sources [1]. To reduce CO_2 emissions, part of the power production can be substituted by similar thermochemical technologies, such as gasification, where a solid fuel is converted into a gaseous one referred to as product gas, allowing its use more efficiently in combined power cycles. Nevertheless, biomass gasification suffers from some technical problems prohibiting the economical and trouble free operation of numerous power stations conceptually based on its advantages.

One of the most commonly studied and applied biomass gasification technology involves processing the solid fuel in a fluidised bed (FB) reactor. FB gasifiers are considered a suitable solution for biomass throughputs above 5 MW_{th} [2]. During the past decade several FB biomass gasifiers were reported in design phase or already operating on a demonstration or (semi-) commercial scale worldwide [3,4]. FBs are relatively fuel-flexible concerning the feedstock's particle size and moisture content but suffer from two major problems: a generic problem associated with increased tar content in the product gas that inhibits its smooth utilisation and a fuel-specific problem, which is examined in the present study, deriving from the low melting temperatures of biomass ashes that create particle sintering, agglomeration, and eventually defluidisation of the FB.

Biomass fuels, especially those stemming from herbaceous plants, contain silicon, potassium, sodium and alkali earth metals as principal ash forming constituents, together with chlorine and sulphur to a lesser extent [5–7]. The formation of low melting ash derived compounds such as alkali silicates creates problems in FB reactors at high temperatures; the formation of sticky glassy melt causes bed particle agglomeration. The growth and accumulation of agglomerates may lead to a loss of fluidisation (defluidisation) and unscheduled shutdowns. The problem is common to both combustors and

* Corresponding author. Tel.: +30 210 7722810; fax: +30 210 7723663.
E-mail address: lfryda@central.ntua.gr (L.E. Fryda).

0032-5910/$ - see front matter © 2007 Elsevier B.V. All rights reserved.
doi:10.1016/j.powtec.2007.05.022

gasifiers operating at 750 °C–900 °C and its prediction and tackling requires a better understanding of its mechanisms.

The objective of the present work is to study the agglomeration phenomena of three promising biomass fuels in two commonly used bed materials i) quartz sand and ii) olivine, which is a natural material active in reducing the tar content of the product gas. The fuels chosen were two energy crops, namely a) Giant Reed, and b) Sweet Sorghum bagasse, as well as an agro industrial residue: c) olive bagasse. These represent some of the most promising solid biofuels in southern Mediterranean regions. For all the fuel and bed material combinations, externally induced fluidisation loss experiments were conducted in a lab-scale fluidised bed gasifier. Coatings and necks of melt between agglomerated particles were analysed with SEM/EDS. These chemical analyses were compared with chemical equilibrium modelling predictions of the developed chemical system in the FB (ash and gasification atmosphere).

2. Literature survey on sintering and agglomeration phenomena in FBs

2.1. Bed sintering in FB

The early work of Gluckmann et al., cited by Kunii and Levenspiel [8], experimentally demonstrated that the minimum fluidisation velocity will not follow Ergun's equation but increase sharply with temperature above a certain value which they named 'initial sintering temperature'. Comparatively they observed that addition of a liquid (viscous phase) into a gas fluidised bed led to defluidisation by making particles more cohesive.

At elevated temperatures, Seville et al., [9], described sintering in an FB as a time dependent interparticle process in which particle material migrates to regions of particle to particle contacting by mechanisms of a) diffusion, b) viscous flow or c) a combination of the two; leading to the formation and gradual growth of necks. Defluidisation occurs when these necks grow to a point that they are strong enough to withstand the disruptive forces in the fluidised bed [10]. In the presence of ash material in a high temperature FB, sintering is promoted by low melting point eutectics forming a liquid phase.

2.2. Sintering/agglomeration in FB thermochemical processing of solid fuels

There are several reported works on ash related sintering and agglomeration in FBs performing combustion or gasification. According to Skrifvars et al. [11], three sintering mechanisms are identified in solid fuel FBs: a) partial ash melting; b) partial melting with the formation of a viscous liquid (viscous flow sintering); and c) chemical reaction forming a layer of a new compound on particles. The dominant mechanism depends mainly on the chemical and mineralogical composition of the ash involved.

In coal fired FB installations, the agglomeration is predominantly the result of partial melting or chemical reaction of ashes gluing particles together [11]. The latter occurs in desulphurisation processes, when CaO from the ash or from added dolomite and gaseous SO_2 are present. Viscous flow sintering mechanism occurs in silicate systems especially with alkali rich fuels such as biomass. Ash derived alkalis deposit on the bed material or silicate ash particles as (i) small particles, (ii) condensation of alkali species (KCl, KOH, K_2SO_4, K), or (iii) chemical reaction with particle surface followed by homogenization and strengthening of the inner layer of the coating that finally leads to melting and adhesion increase, responsible for the agglomeration result [12–14]. This surface liquid phase is usually highly viscous that even if temperature falls below its solidus value, it remains as a glassy phase. Its viscosity depends on the chemical composition and temperature, and together with time they have been shown to control the neck formation in viscous flow sintering. The Frenkel model can be used for describing this mechanism [15,16,9], in relation to fly ash properties [13]:

$$x(t)^2 = \frac{3r\gamma t}{2\eta}$$

where γ the surface tension of the viscous phase, x the equivalent surface area (neck) between particles, η viscosity of melt, t time, r radius of particles.

Visser [17] summarised two major pathways towards agglomeration that are coherent with the above mentioned discussion: "melt-induced" and "coating-induced" agglomeration. In the first, bed particles adhere together by a molten phase due to local peak temperatures, the chemical composition of which resembles that of ash. "Coating-induced" agglomeration is considered to be more common; a coating layer on particles is formed, that given certain critical conditions (e.g., temperature and thickness), can form necks between individual grains. Partial defluidisation is followed by local regions of high temperatures where melt formation may occur and agglomeration proceeds with both pathways.

2.3. Experimental investigations of agglomeration in FB combustors/gasifiers

Several experimental works examining agglomeration during fluidised bed combustion/gasification of coal and/or biomass are available based on lab or pilot scale FB systems [18–24]. Such works are often accompanied by SEM/EDS analyses of bed particles and agglomerates studying their morphology and composition. Öhman and Nordin [25] systematically experimented on the agglomeration behaviour of different biomass ashes in a lab-scale FB combustor and determined the defluidisation temperature by increasing the bed temperature in a controlled manner. The result was found to be close to the initial sintering temperature of the ash determined with the compression strength method. The coating compositions were dominated by potassium, calcium and magnesium silicates and sometimes inward chemical attack was observed, in addition to the common sticky coating or neck formation that caused agglomeration of particles [26]. Another work from

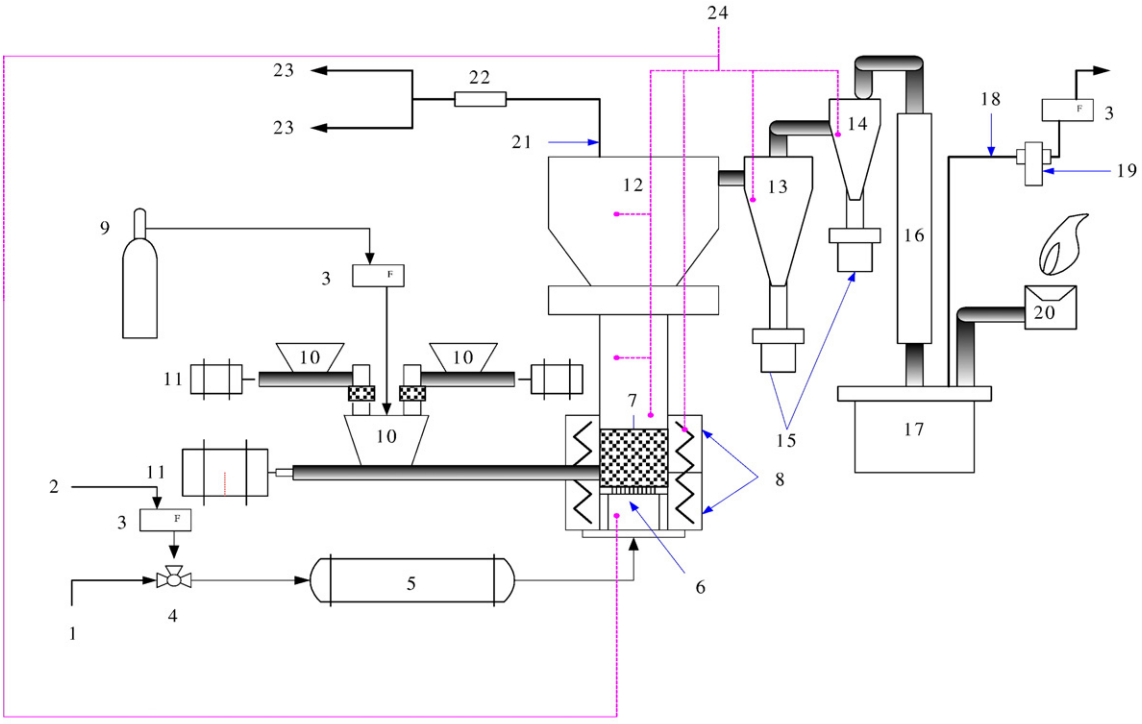

1	Pressurised air flow	13/14	primary/secondary cyclone
2	Alternative input (e.g. steam)	15	Ash collection bin
3	Air/N_2/steam/flue gas mass flow meter	16	Gas cooler
4	Steam – air valve distributor	17	Condensate collector
5	Preheater	18	Sampling line for GC
6	Distributor	19	Filter
7	Fluidised bed	20	Product gas destruction system (flare)
8	Electric resistance	21	Heated sampling probe
9	N_2 flow for backflow prevention	22	Heated ceramic filter
10/11	Fuel silo / Inverter/electric motor	23	Tar measurement
12	Freeboard	24	PC/data collection system

Fig. 1. The lab-scale bubbling fluidised bed gasification reactor.

Öhman et al, [27] compared the elemental compositions of particle coatings between biomass FB gasification and combustion and found no differences in their compositions although gasification coatings were developed to a lesser thickness.

2.4. Prediction and prevention of agglomeration

The purpose of laboratory experimental and theoretical investigations on FB agglomeration is to establish predicting methodologies for assessing the tendency towards agglomeration of new fuels and to find ways of tackling the problem.

Proposed analytical methods [28,29] for predicting the ash sintering behaviour can be: a) fuel analyses: slagging/fouling indices derived from standard ash chemical composition (relation of alkaline earth oxides to alkaline oxides), chemical fractionation [14], and b) determination of ash melting, sintering, and agglomeration temperatures such as the ASTM ash fusion test, differential thermal analysis/thermogravimetric analysis, thermo mechanical tests such as pressure strength measurement of heated ash pellets, shrinkage analysis, etc. Nevertheless, these laboratory analytical methods have been poor indicators since laboratory produced ash is different from an actual FB combustion or gasification process and important factors for the agglomeration process such as particle partitioning, gas solid reactions, or re-condensation of alkali vapours on fly ash are not taken into account. That is why reliable results have been obtained practically only from actual fluidised bed tests. The controlled bed agglomeration test [30] gives the best predictions, since it imitates the actual large scale process.

Reported theoretical studies on the agglomeration process focus on thermodynamic equilibrium calculations to determine the ash derived alkali chemistry behaviour [29,31]. As thermodynamic calculations suffer from their inherent assumption of infinite residence times, they can only be used as a supplement to experimental efforts or guides to develop solutions to the problem.

Some methods to increase the sintering temperature and reduce the amount of melt produced in FBs have been proposed. Silica sand does not hinder agglomeration, in contrast to materials like kaolin or lime that are reported to improve the

situation by chemically interacting with low temperature eutectics, increasing their melting temperatures [32,33]. Using alumina sand as a bed material, the FB can operate smoothly at temperatures as high as 900 °C without any agglomeration or slag problem [20,34,35]. The addition of alkali earth metals (Mg, Ca) inhibits agglomeration by decreasing the melt fraction at elevated temperatures [36].

3. Experimental section

3.1. Experimental set up

A schematic of the experimental atmospheric FB gasifier used for the defluidisation experiments is shown in Fig. 1. The reactor is a stainless steel cylindrical tube of 8.9 cm ID and 1.3 m height, placed in an electrically heated oven with radiative electric resistances applied to preheat and make up for heat losses in the bed. The gasification/fluidising air was preheated and introduced into the reactor through a perforated plate type distributor. The bed consisted of 2000 g material, quartz sand or olivine. The fuel was fed from a silo through a screw feeder into the bed, 8 cm above the air distributor plate. A nitrogen overpressure was introduced to the silo to avoid gas back flow. The pressure losses across the bed were constantly monitored with a differential pressure transducer. When the pressure difference was reduced, this was evidence of agglomeration and defluidisation (creation of gas channels within the bed). Several type K chromel–alumel thermocouples were used to measure temperatures with an accuracy of ±5 °C along the bed, freeboard etc. Due to poor mixing, when the bed was partially defluidised, the temperature profile was not homogeneous. Bed temperature profiles, pressures, and gas flows were monitored and logged on a PC via a data acquisition unit.

3.2. Biomass fuels

Three different biomass fuels were examined: Giant Reed, Sweet Sorghum bagasse, and dried olive bagasse. The first two are energy crops and the third is a very common agro industrial residue, all of which are promising biomass fuels for southern Mediterranean countries. Sweet Sorghum can be primarily utilised for bioethanol production because of its high sugar content [37,38]. Large amounts of fibrous bagasse are the by product of sugar extraction; the dry residue is suitable for thermo-chemical processes such as combustion or gasification. Giant Reed is a proposed future energy crop indented primarily for thermochemical utilisation. It is a widespread, perennial and herbaceous plant, growing spontaneously in Mediterranean regions, with a high aptitude for accumulation of biomass [39]. Finally, considerable amounts of agro industrial residues are available in suitable forms for thermochemical processing: olive bagasse is such an example in Spain, Italy and Greece where it is already being used for heat and power production. There are several reported works examining combustion/gasification of olive bagasse in lab and pilot scale FBs [40–42].

The proximate, ultimate and ash analysis of the fuels are given in Tables 1 and 2. Ca, K and Si account for 90% of the biomass ashes (expressed as oxides). The Si content is high in fast growing and/or annual crops such as the energy crops considered here, while lower for woody biomasses such as the olive bagasse which has higher Ca, Fe, and Al content. The potassium content is high in all three fuels, therefore their thermochemical processing in FB is expected to be problematic to some extent.

3.3. Bed materials

Two different bed materials were used: quartz sand and olivine. Their chemical compositions are given in Table 3. During biomass gasification olivine fluidised beds have proven tar cracking capabilities, mainly attributed to their Fe and Mg content [43,44]. In both cases the initial bed inventory was 2000 g sieved to a narrow particle size distribution and the fluidisation velocity was kept approximately twice the minimum ($U/U_{mf} \approx 2$). This way the onset of particles agglomeration causes a more distinct fluidisation loss that can be conveniently determined when bed pressure difference is suddenly reduced [25,45]. The particle size distribution of the bed after the defluidisation was also determined for every trial.

3.4. Defluidisation trials and bed material SEM/EDS analysis

Externally induced agglomeration/defluidisation tests were performed for each combination of the above mentioned fuel and bed material at air stoichiometry $\lambda = 0.3$. The gasifier operated at moderate temperatures (below 800 °C) for several hours, until biomass ash accumulation in the bed was around 1.5 wt.%. Then the reactor's temperature was gradually raised by providing heat externally, with heating rate approximately 1.5 °C/min, and the temperature at which defluidisation occurred was determined by the sudden FB bed pressure difference drop. Table 4 gives the gasification duration (hours) and average temperature (°C, accuracy ±3 °C) prior to the defluidisation trials onset. The exact feeding rate depended on fuel characteristics (stickiness, ability to flow smoothly, cavitation formation) therefore it differed from fuel to fuel. In

Table 1
Proximate and ultimate analysis of the fuels

Parameter	Giant Reed (*Arundo Donax* L.)	Sweet Sorghum bagasse	Olive bagasse
Proximate analysis (wt.%)			
Moisture	7.4	8.1	8.8
Ash	2.48	3.2	2.4
Ultimate analysis (wt.%, dry basis)			
C	46.5	49.5	51.3
H	5.7	6.2	5.8
N	0.5	0.9	1
S	0.01	0.01	0.0
O [a]	44.7	40.1	39
Ash	2.6	3.3	2.6
HHV d.b (kJ/kg) [b]	17 980	18 322	19 840

[a] By subtraction.
[b] Higher heating value (HHV) of dry solids (d.b.).

Table 2
Chemical analysis (wt.%) of the fuels' ash

Compound	Giant Reed (*Arundo Donax* L.)	Sweet Sorghum bagasse	Olive bagasse
SiO_2	44.2	31.6	26.4
Al_2O_3	1.8	1.9	4.8
Fe_2O_3	0.9	0.4	7.3
CaO	1.8	10.9	27.1
MgO	2.8	6.3	4.7
TiO_2	0.1	–	0.3
Na_2O	0.5	0.2	–
K_2O	30.0	31.6	25.8
P_2O_5	3.2	3.8	2.6
Cl	–	5.1	–

order to achieve 1.5% w/w ash accumulation, operation duration was calculated and then applied. In several cases, due to strong feeding fluctuations, this estimated value was not correct, resulting in unexpected earlier defluidisation or unexpectedly high defluidisation temperatures. None of these trials was included in the work. Table 4 presents average values obtained from three daily trials. In case one value was considerably different from the other two it was not included, and the experiments were repeated. The total duration of this experimental work lasted from May until mid September 2005 and SEM analyses took place from September until end November. A typical gasification curve, showing pressure difference ΔP and temperatures T within the bed vs. time during a daily test is given in Fig. 2. Once defluidisation started, poor bed mixing caused an inhomogeneous bed temperature profile apart from the significant pressure drop, and temperature increased at the upper FB section. After bed defluidisation the reactor was turned to nitrogen flow, cooled, and the bed material was collected and sieved to determine the new particle size distribution.

Several samples of bed agglomerates were collected and characterised with Scanning Electron Microscopy (SEM) combined with Energy Dispersive Spectrometry (EDS). Spot chemical analyses on agglomerates and their cross-sections were performed in order to study the distribution of several important ash elements on the particle coatings responsible for the agglomeration.

4. Equilibrium calculations for evaluation of the ash melting behaviour

An effort was made to compare the experimental results on defluidisation temperature and ash coating compositions with predictions from chemical equilibrium modelling for each fuels' ash in the presence of product gas and significant excess of bed material. For this purpose the equilibrium module of FactSAGE™ software was used, based on the Gibbs' free energy minimisation using the SGTE thermodynamic database [46].

The main solution phases used in the calculations are shown in Table 5. Two kinds of melt were considered, insoluble to each other [29,31]: a) A salt melt consisting of alkali carbonates, chlorides, and sulphates and b) A slag melt consisting of calcium, magnesium, potassium, sodium, and silicon oxides. Aluminium oxide (Al_2O_3) was not taken into account because its presence in the chemical equilibrium calculations resulted in very low melting point estimations (even below 700 °C). The same assumption was made by [36]. This observation contradicts other studies concluding that alumina beds increase the system melting temperatures [34,35].

The calculations were based on the major biomass elements: C, H, N, O, S, and the ash constituents: K, Mg, Si, Cl, Ca, Fe. All fuel and bed material compositions were taken from the composition analyses given in Tables 1, 2, and 3. The ash load of the bed was set to 1.5 wt.% (a value based on the experimental trials). For atmospheric pressure and air stoichiometry of 0.3, the equilibrium was evaluated for temperatures between 700 and 1200 °C. The results included the amounts and main compositions of the dominant phases. Since potassium silicates are responsible for low temperature eutectics, the presented results focus on the thermodynamically predicted fate of potassium.

5. Results and discussion

5.1. Defluidisation temperatures

The defluidisation temperatures determined at the onset of ΔP_{bed} drop had an accuracy of ±3 °C. The results, the mean values of which are shown in Table 6, reveal that Giant Reed had the highest agglomeration tendency followed by Sweet Sorghum bagasse and lastly olive bagasse. The defluidisation temperature in olive bagasse gasification is even higher when olivine bed material is used. This can be attributed to the lower potassium and silicon and higher calcium and iron in its ash, in combination with the presence of Mg in the olivine bed material.

5.2. Bed material characterisation

The bed material PSDs before and after each test are shown in Fig. 3, where the shift towards larger diameters is evident. In

Table 3
Chemical composition and density of the bed materials used

	Fraction (wt.%)	
Compound	Olivine	Sand
SiO_2	47–49	99%
FeO	7–8	–
MgO	41–42	–
$Cr_2O_3+NiO+CaO+Al_2O_3$	<1	~1
Density (kg/m^3)	3200	2600

Table 4
Duration and temperature of biomass gasification prior to defluidisation trials

	Giant reed (*Arundo Donax* L.)	Sweet sorghum bagasse	Olive bagasse
Feeding rate		Duration (h)/temperature (±3 °C)	
200 g/h	–	5.5–6.0/770	–
400 g/h	3.8–4/770	–	4.0/800
490 g/h	3.0–3.5/770	–	3.0/800

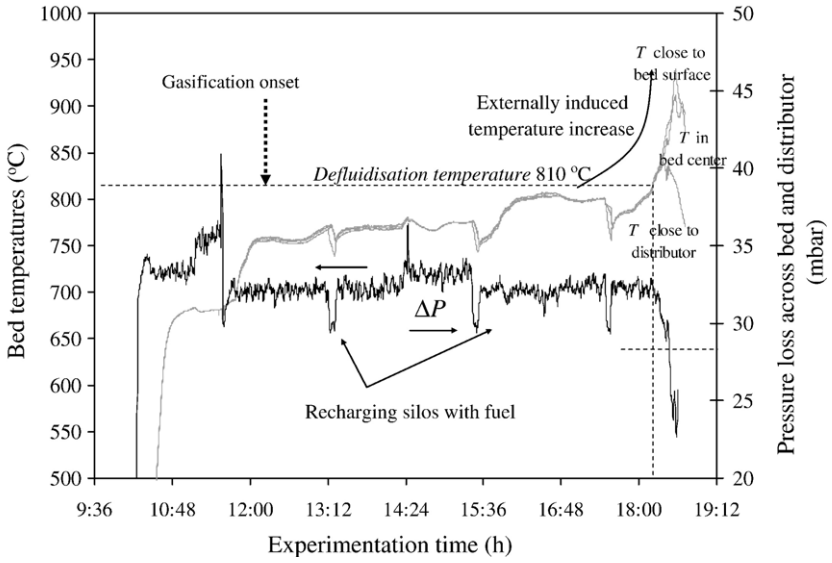

Fig. 2. Typical bed pressure loss and temperature monitoring during defluidisation test (Sweet Sorghum bagasse in quartz bed).

all tests the smaller sized particles of the original bed were almost completely combined to larger particles. Numerous SEM/EDS analyses where performed on agglomerates and their cross-sections. Some of the most representative and explanatory SEMs are discussed in the following paragraphs.

Table 5
Summary of solution phases included in the thermodynamic analysis [46]

Solution species	Components in the solution species used in modelling	General comments on solution type (available compounds)
FACT–MeO	CaO, MgO	Solid solution
FACT–SLAG (A–F)	MgO, SiO_2, CaO, K_2O, MgS, CaS, $CaSO_4$, $MgSO_4$	Slag/liquid Si rich solution, Al, As, B, Ca, Co, Cr, Cu, Fe, Ge, K, Mg, Mn, Na, Ni, Pb, Si, Sn, Ti, Zn, Zr; dilute S, SO_4, PO_4, H_2O/OH, CO_3, F, Cl, I Selection refined according to input compounds
FACT oPyr/cPyr/LcPyr/pPyr	$CaMgSi_2O_6$, $Mg_2Si_2O_6$	Orthopyroxene, solid solution
FACT WOLL	$MgSiO_3$, $CaSiO_3$	Solid solution
FACT Oli	$CaMgSiO_4$, Ca_2SiO_4, Mg_2SiO_4	Solid solution
FACT SALT (A–F)	KCl, KOH, KNO_3, K_2SO_4, K_2CO_3	Liquid solution Li, Na, K, Mg, Ca, Mn, Fe, Co, Ni, Al, Rb, Cs//Cl, F, Br, I, NO_3, OH, SO_4, CO_3 (dilute; O,OH)
FACT LCSO	Liquid K_2SO_4, $CaSO_4$, K_2CO_3,$CaCO_3$	Liquid sulphate solution, K, Ca//CO_3, SO_4 Molten reciprocal solution K_2CO_3–K_2SO_4–$CaCO_3$–$CaSO_4$.
FACT SCSO	K_2SO_4,$CaSO_4$, K_2CO_3, $CaCO_3$	Solid solution
FACT SCMO	Solid-Ca(SO_4), Mg(SO_4)	Solid solution
FACT LSUL	Liquid-Ca, Mg/(SO_4)	Liquid sulphate solution $CaSO_4$–$MgSO_4$–Na_2SO_4

An interesting agglomerate shape was common in the tests of Giant Reed and Sweet Sorghum, appearing as longish clusters of particles bound together. Similar agglomerates were observed by Öhman and Nordin [45]. SEM images of such agglomerates are shown in Fig. 4, obtained from the Giant Reed gasification in quartz (Fig. 4a), and olivine (Fig. 4b) and Sweet Sorghum bagasse gasification in olivine (Fig. 4c). A typical SEM cross-section of a cluster-like agglomerate from the Giant Reed gasification test in quartz sand is shown in picture (Fig. 4d), revealing the mechanism of its formation: its centreline is composed of a thin long ash particle that is the remaining of a fuel char particle. Giant Reed followed by Sweet Sorghum bagasse have a very high alkali and silicate ash content that can easily melt at the elevated temperatures of a reacting char particle. This makes the char very adhesive and prone to capture bed material grains. It has to be noted that this was not noticed in the olive bagasse tests.

Fig. 5 shows four SEM photographs of bed material particles significantly covered with ash melt gluing them together. The numbering corresponds to spot EDS composition analyses given in the accompanying bar graphs. The photograph in Fig. 5a, shows an agglomerate from the olive bagasse experiments in quartz sand covered with ash coating rich in potassium, silicon and to a lesser extent calcium, iron and aluminium; all deriving from the olive bagasse ash. Calcium presence in the melt can justify its higher defluidisation temperatures (Table 6) [36]. The photograph in Fig. 5b is a cross-section of an agglomerate from the Giant Reed

Table 6
Agglomeration temperatures (°C) as observed from the trials

	Giant reed (*Arundo Donax* L.)	Sweet sorghum bagasse	Olive bagasse
		Defluidisation temperature (±3 °C)	
Quartz	785	810	830
Olivine	790	812	>850

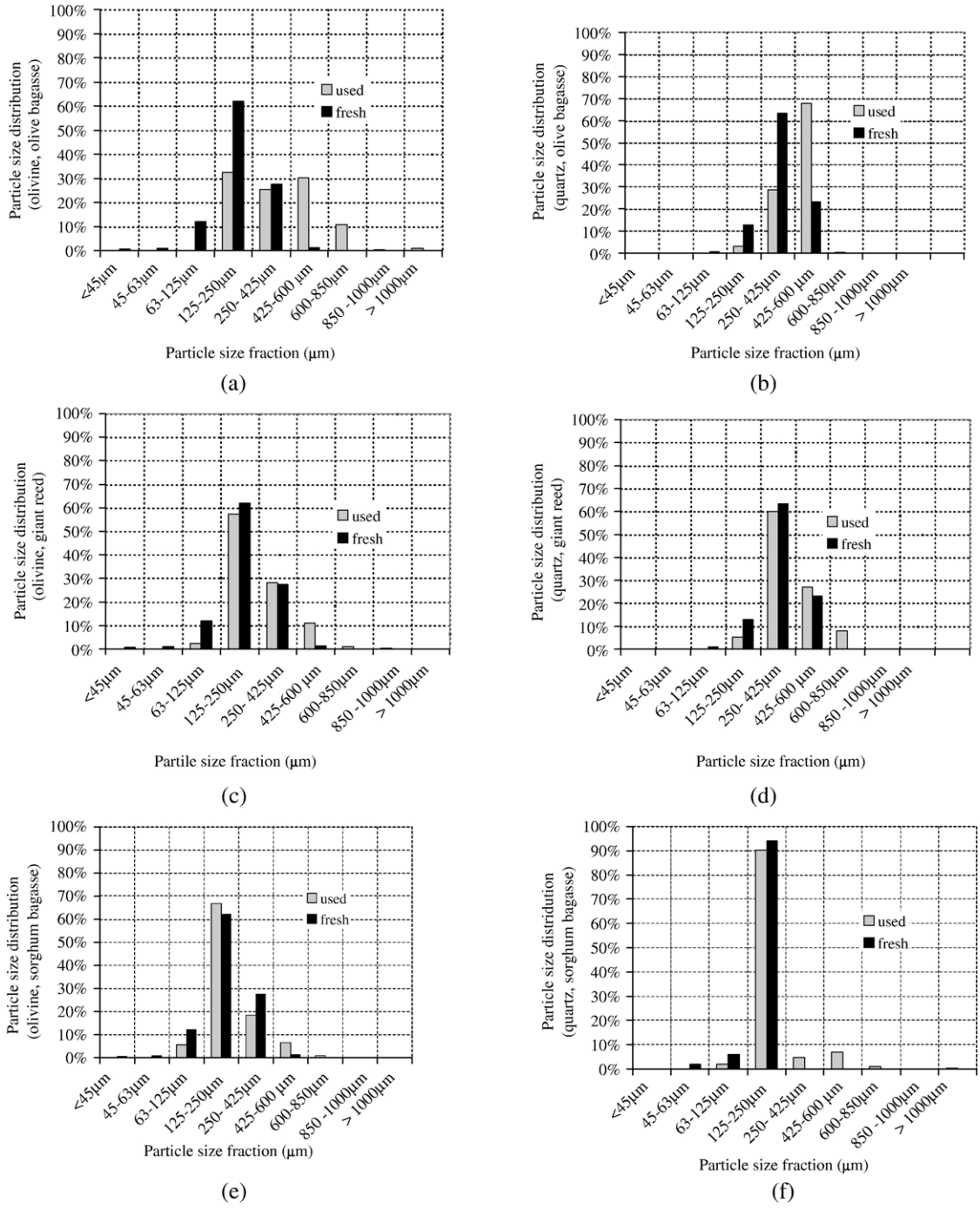

Fig. 3. Particle size distribution of bed material before and after defluidisation tests.

gasification test in quartz, where original bed particles are trapped in potassium silicate melt. Giant Reed bed defluidisation occurred at the lowest temperatures compared to the rest of the trials. The agglomerate in Fig. 5c from the Sorghum/olivine trials, the spot analyses on the melt surrounding the glued particles show potassium silicates and limited Ca from the fuel's ash. The corresponding defluidisation temperature was moderate (Table 6). Finally the photograph in Fig. 5d shows a cross-section detail of a larger agglomerate from olive bagasse tests in olivine.

Agglomerates were also found to be created by neck formation in the particles' contacting regions; examples are shown in Fig. 6. SEM photographs (Fig. 6a–d) show cross-sections of bed particles combined with potassium silicate necks from the Giant Reed tests in quartz (Fig. 6a), Sorghum bagasse in quartz (Fig. 6b) and Sorghum bagasse in olivine (Fig. 6c). Agglomerates with necks were usually composed of two or sometimes three particles; it was very rare that a neck-supported agglomerate comprised of a larger number of particles. An example of such an agglomerate without any ash filling up the

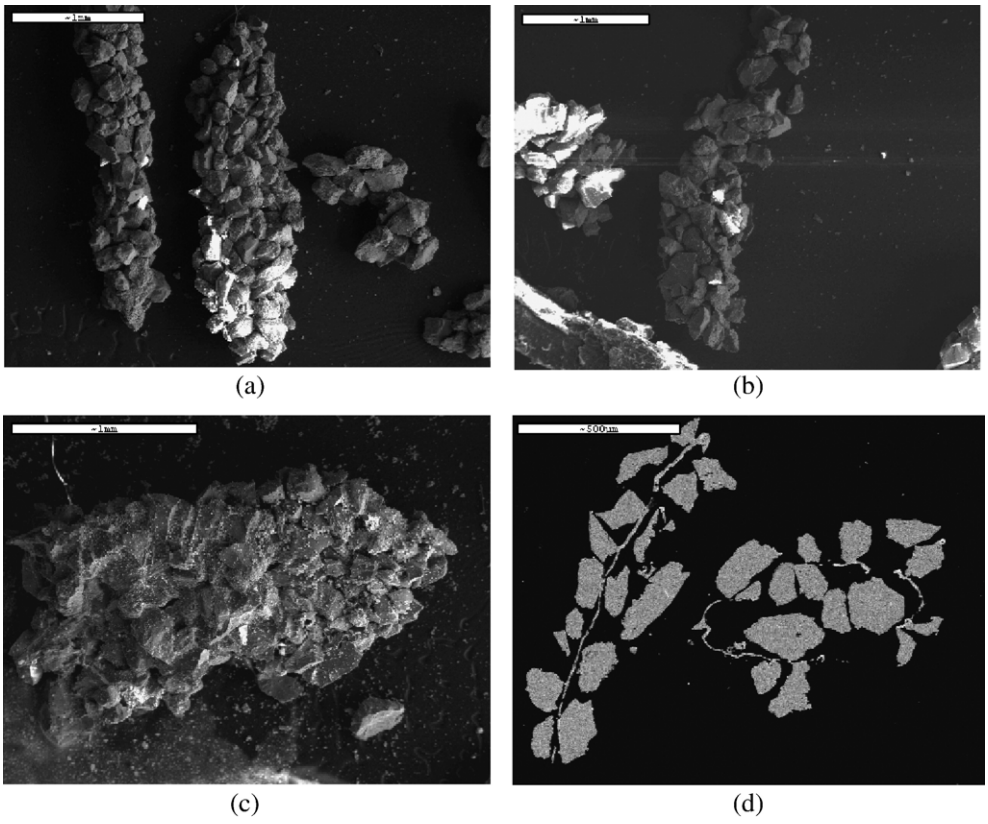

Fig. 4. (a) (b) (c) (d). SEM/EDS photographs of agglomerates from air gasification of Giant Reed in (a) quartz, (b) in olivine, (c) Sweet Sorghum test in olivine and (d) agglomerate cross-section from Giant Reed test in quartz sand.

space surrounding the particles is shown in photograph (Fig. 6d), from olive bagasse gasification in olivine. The spot analyses are shown in accompanying bar graphs in Fig. 6 on the participating particles (numbers 7 to 10) show that the original olivine material is not covered completely with potassium silicate melt (MgO and Fe_2O_3 are present with high concentrations close to that in Table 3 for fresh olivine). Potassium silicate melt is only evident in specific contacting points between particles (i.e. spot analysis 11).

No chemical attack (cracks or evidence of gradual inward reaction propagation) was noticed on the original grains; so the bed material is assumed to participate only to a minor extent in the formation of sticky layers. This is also supported by the fact that there was no significant difference in the agglomeration temperatures between sand and olivine beds with the two herbaceous high potassium ash fuels. Hot spots cannot be prohibited of course; in that case bed material can soften and directly interact with alkali vapours forming eutectics. An explanation for the higher defluidisation temperature of olive bagasse in an olivine bed is attempted in Section 5.4.

5.3. The effect of timescale

Different agglomeration routes are suggested in literature and are summarised in [27]: (i) "melt-induced" agglomeration, for bed materials directly glued together by a separate ash derived melt phase, and (ii) "coating-induced" agglomeration, for the sequential process of coating formation on the bed particles, followed by adhesion and agglomeration. Coating formation requires a certain residence time to develop as it includes chemical reactions between ash and bed material, depending on the physical properties of the bed material itself. On the other side, the rapid formation of ash melt in the bed causes bed particles to stick together directly without forming any coatings. As soon as the temperature in the bed reaches the melting point of ash, defluidisation occurs rapidly, and no coating layers can be formed any more. Therefore, timescale has an effect on the second proposed mechanism (ii). In conclusion, it is the bed temperature that determines whether coating or melt in sufficient quantities is first formed.

A thorough investigation of agglomeration tendency in relation with the time before defluidisation is detected is presented in [24]. As temperature increases, the stickiness of the ash melt increases leading to short defluidisation times. For the same gas velocity and combustion temperature, an increase of particle size leads to a shorter defluidisation time due to the lower specific outer surface area resulting in a thicker ash coating layer.

An extensive experimental study on coating formation on bed particles with time is given in [17], for a variety of fuels and bed materials. The authors also conclude that the quantity and stickiness of a K/Si composition determine whether agglomeration is likely to occur before any outer coating can form (sintering due the formation of a molten ash phase).

As concluded in the previous paragraph, in our experiments, bed particles do not seem to react chemically with ash. The

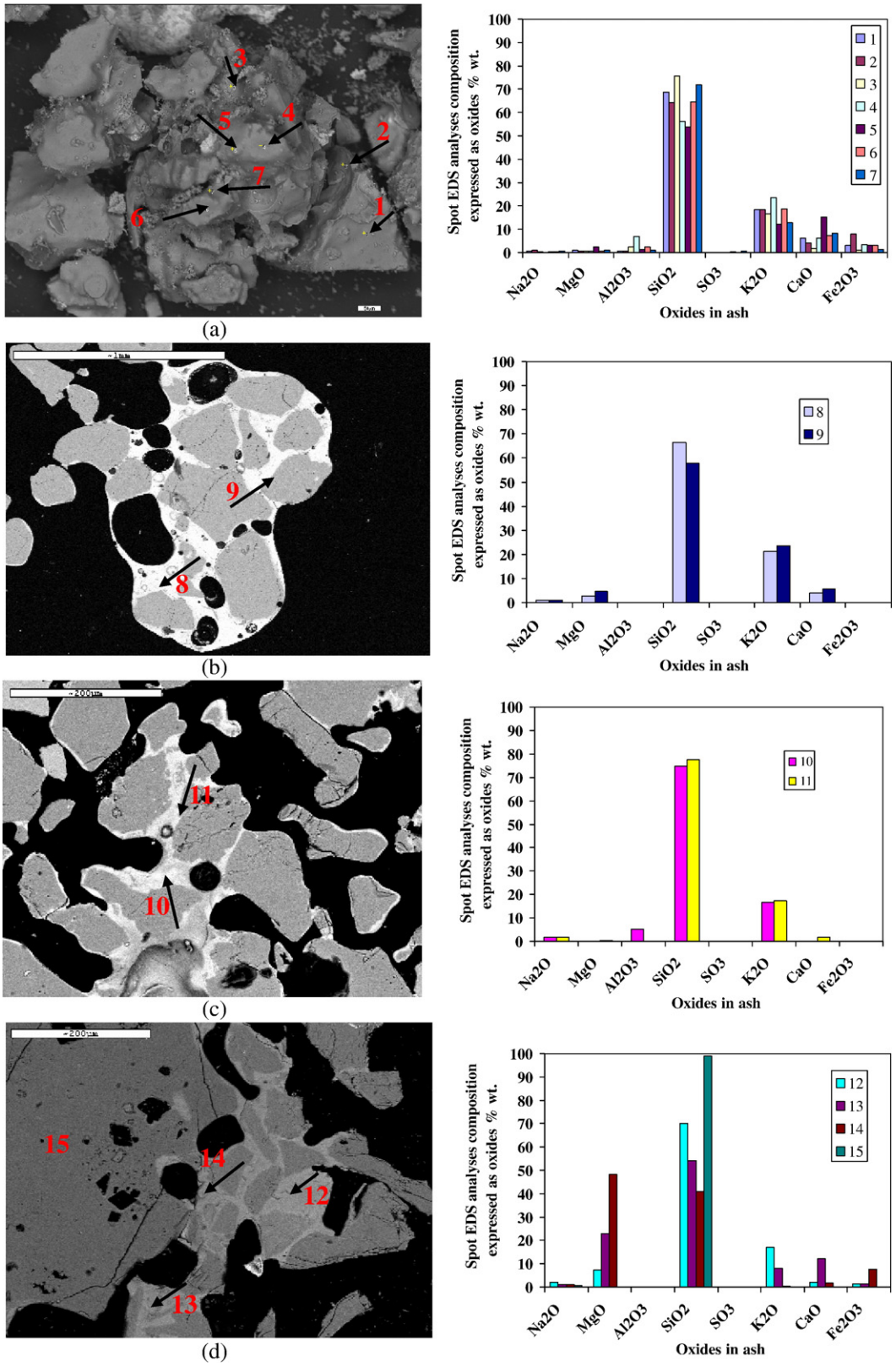

Fig. 5. (a) (b) (c) (d). SEM photograph and EDS analysis of an agglomerate from air gasification of (a) olive bagasse in quartz, agglomerate cross-sections from (b) Giant Reed test in quartz, (c) Sweet Sorghum test in olivine and (d) olive bagasse test in olivine.

dominant mechanism is ash release from fuels reaction, ash melting and sticking of the melt on the surrounding bed particles, which happens very fast. In the case of chemical reaction between ash and bed material, e.g. desulphurisation in limestone bed, the particles react directly with the fuel. This is attributed mainly to the physical characteristics of the particle:

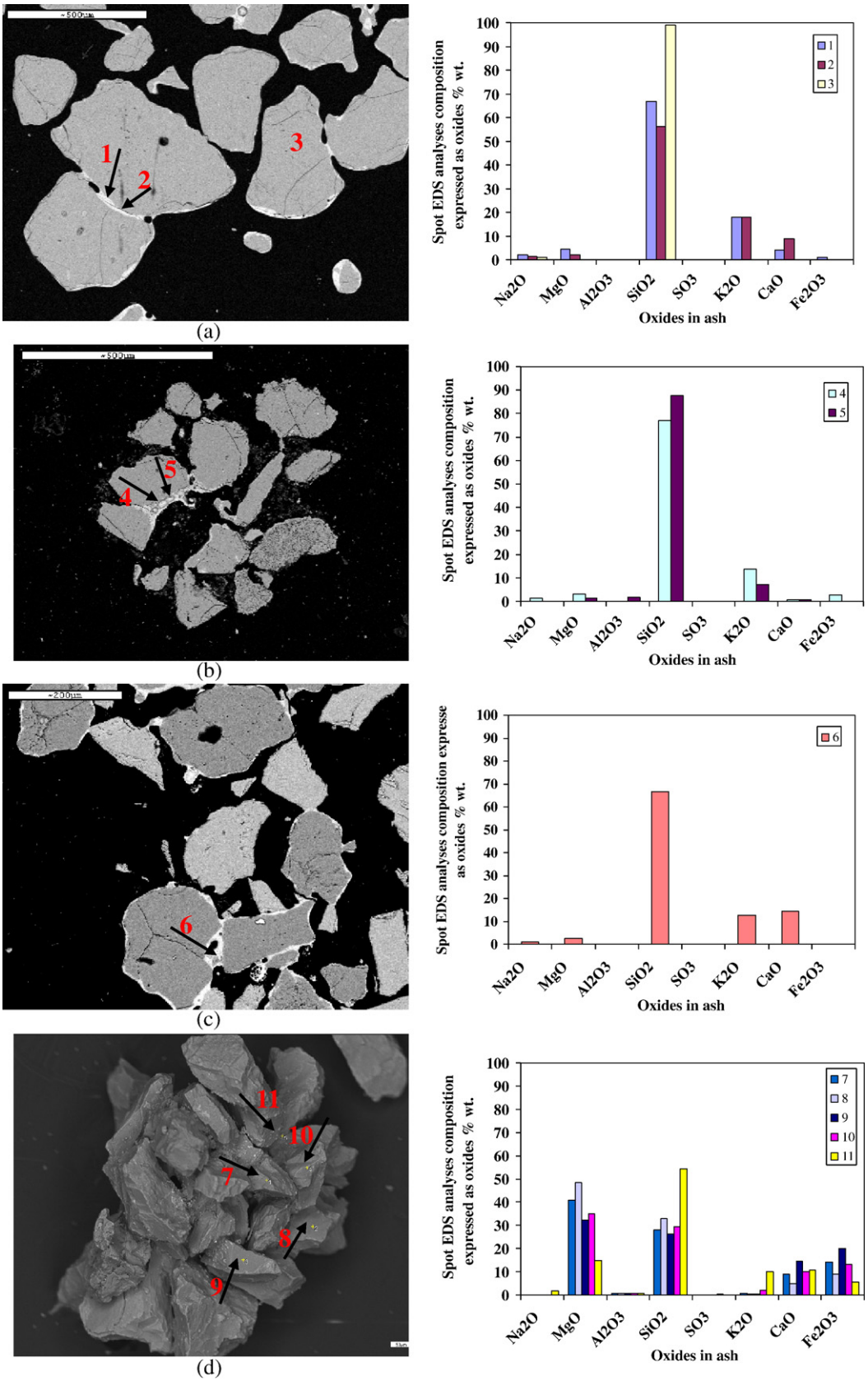

Fig. 6. (a) (b) (c) (d). SEM photograph and EDS analysis of agglomerate cross-sections from air gasification of (a) Giant Reed test in quartz, (b) Sweet Sorghum test in quartz, (c) Sweet Sorghum test in olivine and (d) an agglomerate from the olive bagasse test in olivine.

the CaO which is formed after limestone calcination is highly porous and therefore active.

Some longer tests were performed resulting in higher ash accumulation in the bed (above 1.5% w/w ash) by lowering the operating temperature. In these cases tar formation problems are severe; besides, it was observed that defluidisation was very rapid after reaching a certain temperature. Nevertheless this temperature did not differ significantly from the one determined with 1.5% w/w ash. In a future work some more tests with a greater history of bed particles will be made. In the present paper a common starting point had to be decided to explore the effects of ash content/bed material type.

5.4. Thermodynamic modelling results

5.4.1. Total melt formation calculations

Figs. 7 and 8 for quartz and olivine bed respectively, show the thermodynamic prediction for melt formation in % percentage wt of melt in the total bed inventory as a function of bed temperature in an FB gasifier ($\lambda = 0.3$) of 2000 g (equal to the quantity used in the experiments) with an 1.5 wt.% accumulation of fuel ash for the three biomass fuels.

The exact defluidisation temperature determined experimentally was slightly higher than the initial melting temperature predicted from thermodynamics probably because a critical amount of slag has to become available first. The amount of slag predicted sharply increases with temperature beyond the initial melting temperature.

Thermodynamics predict that Sorghum ash melt appears at slightly lower temperatures compared to the other two fuels but eventually Giant Reed ash yields greater slag quantities in both quartz and olivine beds. Therefore Giant Reed's actual lower defluidisation temperature can be explained by assuming that the critical issue for defluidisation is the amount of ash slag formed. Due to Sorghum's chlorine content, $KCl_{(l)}$ appears in the predictions (Figs. 7 and 8) in small amounts; nevertheless, no chlorine was present in the particle coatings examined. Chlorine is known to act as an alkali facilitator, and could have

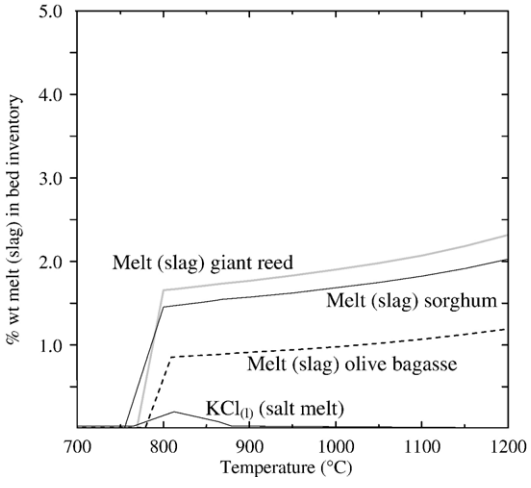

Fig. 7. Melt (slag) percentage (wt.%) as a function of temperature for the three fuel ashes in a 2000 g quartz bed considering 1.5 wt.% ash accumulation.

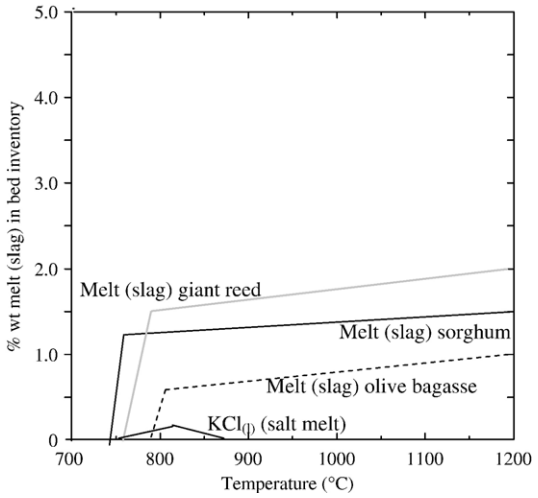

Fig. 8. Melt (slag) percentage (wt.%) as a function of temperature for the three fuel ashes in a 2000 g olivine bed considering 1.5 wt.% ash accumulation.

'carried' potassium to particle surfaces, but it was not bound there eventually.

In the case of olive bagasse, melt formation is predicted at higher temperatures and the melt quantity is considerably less. This is attributed to its lower potassium and higher calcium content compared to the other two fuels. In all three fuels, the amount of slag predicted in quartz sand beds is slightly higher compared to the amount predicted with olivine, probably because of more SiO_2 available to form potassium silicates.

Calculations show that almost all sulphur was released in the gaseous phase as H_2S while only traces of sulphides and sulphates were predicted; by observing the SEM/EDS analyses sulphur also appears only in minor percentage in the coatings.

The SEM/EDS analyses, as presented in the previous paragraph, did not show any sign of particle surface 'attack'. This is proof of the fact that there was no chemical interaction between bed material grains and ash or ash melt. The bed material seems to participate only to a minor extent in the formation of sticky layers, which are formed by an external melt layer caused by molten ash. Therefore, equilibrium calculations were repeated without taking into account the bed material and using as input the same ash quantity as used in the initial runs (ash 1.5 wt.% of bed material) and of course with the same ash composition over the same temperature range. The results predicted less slag in this case, however the trend of the graphs and the initial melt formation temperatures calculated were the same. The difference in quantity is more significant between the predicted quartz sand bed with 1.5% ash wt than between the olivine bed with 1.5% ash wt. In the case of olive bagasse the differences between taking into account the bed material or not were very small, again being larger in the case of quartz sand bed. These results are summarised in Table 7, where the predicted slag formation is given for every fuel/bed material combination as a mass percentage (%) of the initial results including bed material in the calculations. In all cases the melt predicted without considering bed material is less than the melt predicted when considering bed material (reference case 100% melt).

Table 7
Results in predicted slag formation when not considering bed material as percentage (%) of the initial results including bed material in the calculations

	Giant reed (*Arundo Donax* L.)	Sweet sorghum bagasse	Olive bagasse
Bed material	Percentage of mass of melt formed including bed material (%)		
Quartz	65	55	65
Olivine	75	65	~100

An explanation for this is given. The software does not take into account either residence time or fluidisation conditions, or, most important, the activity of the participating solids, which is affected by porosity and grain size. Quartz bed, and also quartz containing olivine bed, consists of crystalline quartz particles with sizes much larger relative to the ash elements. In other words, the Si in the bed material is not as reactive as the elemental Si in the biomass ash, resulting in different behaviour. In fact, bed material is almost chemically inert in contrast to biomass Si which reacts rapidly with biomass K and Ca. The software does not take this fact into account and calculated the equilibrium of the given chemical system considering all Si input as equally active. Another option would be to allow only a small quantity of sand bed to react chemically and reach equilibrium with the rest of the elements.

If the bed material was very fine or in another chemical formula the experimental results might be different, and closer to the initially calculated (all bed material included).

5.4.2. Potassium chemistry in FB gasification

In the gasification reductive atmosphere, at 700–900 °C and atmospheric pressure, the major potassium stable compounds are $K_2Si_4O_{9(s)}$, $(K_2O{\cdot}SiO_2)_{(l)}$ and $KCl_{(s,l,g)}$, although during the thermodynamic calculations, and according to the possible compounds given in Table 4, minor amounts of potassium can appear in several other forms, such as K_2SO_4 or K_2CO_3. Figs. 9 and 10 show the wt.% of major potassium stable forms for the three fuels examined in quartz and olivine bed respectively.

In the case of Sweet Sorghum, where fuel chlorine exists, thermodynamics predict that the solid salt $KCl_{(s)}$, a stable molecule at lower temperatures, starts to liquefy at temperatures around 750 °C in both bed materials. The temperature window at which liquid $KCl_{(l)}$ is present is narrow since at slightly higher temperatures it exists in vapour form (Figs. 9 and 10). Nevertheless, the amount of $KCl_{(l)}$ is limited compared to the $(K_2O{\cdot}SiO_2)_{(l)}$, which is mainly responsible for ash sintering in the bed.

In olive bagasse tests in olivine bed, calcium is predicted in solid solutions a) together with Mg and Si as $MgOCa_3O_3Si_2O_4$ $_{(s)}$, present throughout the whole temperature range and being 50 wt.% of the total solid mixture formed, and b) with Fe and Si as $Ca_3Fe_2Si_3O_{12(s)}$ being 15 wt.% of the total mixture formed at temperatures up to 850 °C. The existence of these stable solid compounds seems to inhibit the stability of liquid potassium silicate formation, and can explain the higher defluidisation temperatures recorded for olive gasification in olivine.

6. Conclusions

The high potassium content of Giant Reed and Sweet Sorghum bagasse causes formation of melt responsible for total defluidisation in the FB agglomeration trials at relatively low temperatures. The main defluidisation mechanism is total melting of the silicate ash forming a highly viscous liquid. Melts consist mainly of alkali silicates and to a lesser extent of other oxides or alkali salts. Bed particle grains were either adhered to the sticky melt or necked together by a molten layer on their surfaces. This is characteristic for silica systems, and is described as viscous flow sintering. According to the sintering and coating mechanisms described, collisions with the reacting fuel particles may dominate the transfer of K-rich compounds to the bed particle surfaces. No obvious chemical interaction between the bed material and the fuel ash in the gasifier was observed with the SEM/EDS analyses. Nevertheless, some original bed material interaction was evident because of a noticeable difference in the defluidisation temperature of olive bagasse in the two beds.

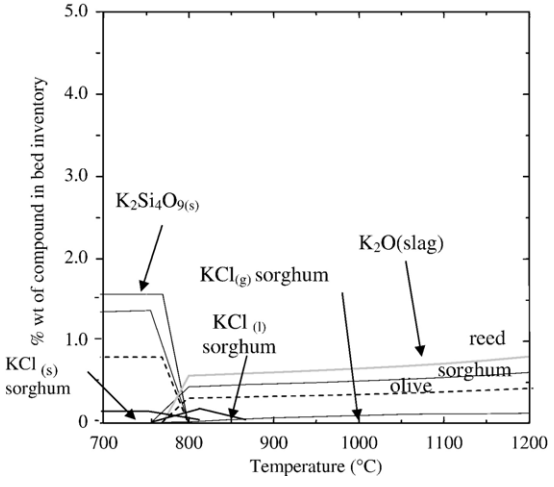

Fig. 9. Major potassium compounds distribution for the three fuel ashes in a 2000 g quartz bed considering 1.5 wt.% ash accumulation.

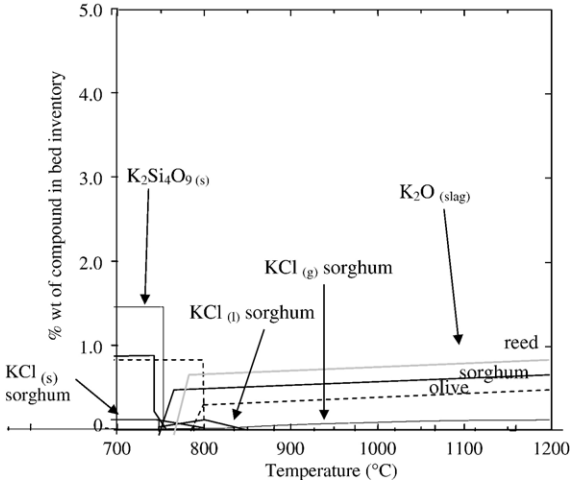

Fig. 10. Major potassium compounds distribution for the three fuel ashes in a 2000 g olivine bed considering 1.5 wt.% ash accumulation.

The amount of predicted melt from thermodynamic calculations is significantly lower in the case of olive bagasse indicating that higher temperatures are necessary to observe defluidisation, which was also confirmed experimentally. Especially in the case of olive bagasse tests in olivine, MgO interacts with the fuel ash and shifts the melting temperature to higher levels.

Acknowledgements

The authors would like to thank Prof. E. Pavlidou of the Scanning Electron Laboratory of the Physics Department at the Aristotle University of Thessaloniki, and Prof. Ch. Katagas of the Geology Department at the University of Patra for their assistance in SEM/EDS imaging.

References

[1] K. Maniatis, E. Millich, Energy from biomass and waste: the contribution of utility scale biomass gasification plants, Biomass and Bioenergy 15 (3) (1998) 195–200.
[2] A.V. Bridgewater, The future for biomass pyrolysis and gasification: status, opportunities and policies for Europe Contract No: 4.1030/S/01-009/2001 Bio-Energy Research Group, Aston University, Birmingham B4 7ET, UK November 2002.
[3] H. Spliethoff, Status of biomass gasification for power production, IFRF Combustion Journal Article 200109, November 2001 ISSN 1562-479X.
[4] C. Higman, M. van den Burgt, Gasification, Elsevier Science, Burlington, 2003.
[5] B. Olanders, B.-M. Steenari, Characterization of ashes from wood and straw, Biomass and Bioenergy 8 (2) (1995) 105–115.
[6] D.L. Klass, Biomass for Renewable Energy, Fuels and Chemicals, Academic Press, 1998.
[7] Alkali deposits found in biomass boilers, NREL/TP-433-8142, Sandia National Laboratory (1998) 206–210.
[8] D. Kunii, O. Levenspiel, Fluidisation Engineering, Second Edition, Butterworth-Heinemann, Boston, 1991.
[9] J.P.K. Seville, C.D. Willett, P.C. Knight, Interparticle forces in fluidisation: a review, Powder Technology 113 (2000) 261–268.
[10] J.P.K. Seville, H. Silomon-Pflug, P.C. Knight, Modelling of sintering of high temperature gas fluidisation, Powder technology 97 (1998) 160–169.
[11] B.J. Skrifvars, M. Hupa, R. Backman, M. Hiltunen, Sintering mechanisms of FBC ashes, Fuel 73 (2) (1994) 171–176.
[12] M. Öhman, A. Nordin, Bed agglomeration characteristics during fluidised bed combustion of biomass fuels, Energy and Fuels 14 (2000) 169–178.
[13] A. van der Drift, A. Olsen, Conversion of biomass, prediction and solution methods for ash agglomeration and related problems, final report, ECN Biomass, 1999.
[14] L. Baxter, T.R. Miles, T.R. Miles Jr., B.M. Jenkins, T. Milne, D. Dayton, R.W. Bryers, L.L. Oden, The behavior of inorganic material in biomass-fired power boilers: field and laboratory experiences, Fuel Processing Technology 54 (1–3) (1998) 47–78.
[15] M.O. Prado, E.D. Zanotto, R. Müller, Model for sintering polydispersed glass particles, Journal of Non-Crystalline Solids 279 (2–3) (2001) 169–178.
[16] M.O. Prado, E.D. Zanotto, Glass sintering with concurrent crystallization, Comptes Rendus Chimie 5 (11) (2002) 773–786.
[17] H.J.M. Visser, The influence of fuel composition on agglomeration behaviour in fluidised-bed combustion, report on the project 'Influence of fuel composition on agglomeration behaviour in fluidised-bed combustion/gasification of biomass', (ECN-C-04-054) Novem subsidy programme, Renewable Energy in the Netherlands, September 2004.
[18] A. Ergüdenler, A.E. Ghaly, Agglomeration of silica sand in a fluidised bed gasifier operating on wheat straw, Biomass and Bioenergy 4 (2) (1992) 135–147.
[19] A. Ergüdenler, A.E. Ghaly, Agglomeration of alumina sand in a fluidised bed straw gasifier at elevated temperatures, Bioresource Technology 43 (1993) 259–268.
[20] A.E. Ghaly, A. Ergüdenler, E. Laufer, Agglomeration characteristics of alumina Sand-straw ash mixtures at elevated temperatures, Biomass and Bioenergy 5 (6) (1993) 467–480.
[21] M.R. Dawson, C.R. Brown, Bed material cohesion and loss of fluidisation during fluidised bed combustion of Midwestern coal, Fuel 71 (1992) 585–592.
[22] A.R. Manzoori, P.K. Agarwal, The fate of organically bound inorganic elements and sodium chloride during fluidised bed combustion of high sodium, high sulphur low rank coals, Fuel 71 (1992) 513–522.
[23] W. Lin, K.D. Johansen, Agglomeration in fluidised bed combustion of biomass — mechanisms and co-firing with coal, ASME Proceedings of the 15th International Conference on Fluidised Bed Combustion, May 16– 19, 1999, Savannah, Georgia, 1999.
[24] W. Lin, K.D. Johansen, F. Frandsen, Agglomeration in bio-fuel fired fluidised bed combustors, Chemical Engineering Journal 96 (2003) 171–185.
[25] M. Öhman, A. Nordin, A new method for quantification of fluidised bed agglomeration tendencies: a sensitivity analysis, Energy and Fuels 12 (1998) 90–94.
[26] E. Brus, M. Öhman, A. Nordin, Mechanisms of bed agglomeration during fluidised-combustion of biomass fuels, Energy and Fuels 19 (2005) 825–832.
[27] M. Öhman, L. Pommer, A. Nordin, Bed agglomeration characteristics and mechanisms during gasification and combustion of biomass fuels, Energy and Fuels 19 (4) (2005) 1742–1748.
[28] M.J. Fernandez Llorente, J.E. Carrasco Garcýa, Comparing methods for predicting the sintering of biomass ash in combustion, Fuel 84 (2005) 1893–1900.
[29] M. Zevenhoven-Onderwater, R. Backman, B.J. Skrifvars, M. Hupa, The ash chemistry in fluidised bed gasification of biomass fuels. Part I: predicting the chemistry of melting ashes and ash–bed material interaction, Fuel 80 (10) (2001) 1489–1502.
[30] B.-J. Skrifvars, M. Öhman, A. Nordin, M. Hupa, Predicting bed agglomeration tendencies for biomass fuels fired in FBC boilers: A Comparison of Three Different Prediction Methods, Energy and Fuels 13 (1999) 359–363.
[31] B.J. Skrifvars, R. Backman, M. Hupa, Characterization of the sintering tendency of ten biomass ashes in FBC conditions by a laboratory test and by phase equilibrium calculations, Fuel Processing Technology 56 (1998) 55–67.
[32] M. Öhman, A. Nordin, The role of kaolin in prevention of bed agglomeration during fluidised bed combustion of biomass, Energy and Fuels 14 (2000) 618–624.
[33] E. Natarajan, M. Öhman, M. Gabra, A. Nordin, T. Liliendahl, A.N. Rao, Experimental investigation of bed agglomeration tendencies of some common agricultural residues in fluidised bed combustion and gasification, Biomass and Bioenergy 15 (2) (1998) 163–168.
[34] J. Baeyens, D. Geldart, Solids mixing, in: D. Geldart (Ed.), Gas Fluidising Technology, John Wiley and Sons, N.Y., 1986, pp. 97–122, Chapter 5.
[35] J. Baeyens, F. Van Puyvelde, Fluidised bed incineration of sewage sludge: a strategy for the design of the incinerator and the future for incinerator ash utilization, Journal of Hazardous Materials 1 (37) (1994) 179–190.
[36] H. Risnes, J. Fjellerup, U. Henriksen, A. Moilanen, P. Norby, K. Papadakis, D. Posselt, L.H. Sørensen, Calcium addition in straw gasification, Fuel 82 (6) (2003) 641–651.
[37] S. Kim, B.E. Dale, Global potential bioethanol production from wasted crops and crop residues, Biomass and Bioenergy 26 (2004) 361–375.
[38] K. Suresh, N. Kiransree, L. Venkateswer Rao, Utilization of damaged sorghum and rice grains for ethanol production by simultaneous saccharification and fermentation, Bioresource Technology 68 (3) (1999) 301–304.
[39] S.L. Cosentino, V. Copani, G.M.D'Agosta, E.S. and M. Mantineo, First results on evaluation of *Arundo donax* L. clones collected in Southern Italy, Industrial Crops and Products, in Press, Available online 24 August 2005.
[40] R.N. Andre, F. Pinto, C. Franco, M. Dias, I. Gulyurtlu, M.A.A. Matos, I. Cabrita, Fluidised bed co-gasification of coal and olive oil industry wastes, Fuel 84 (2005) 1635–1644.

[41] P. Garcia-Ibanez, A. Cabanillas, J.M. Sanchez, Gasification of leached orujillo (olive oil waste) in a pilot plant circulating fluidised bed reactor, preliminary results, Biomass and Bioenergy 27 (2004) 183–194.
[42] L. Armesto, A. Bahillo, A. Cabanillas, K. Veijonen, J. Otero, A. Plumed, L. Salvador, Co-combustion of coal and olive oil industry residues in fluidised bed, Fuel 8 (82) (2003) 993–1000.
[43] T. Nordgreen, T. Liliedahl, K. Sjöström, Metallic iron as a tar breakdown catalyst related to atmospheric, fluidised bed gasification of biomass, Fuel 85 (5–6) (2006) 689–694.
[44] L. Devi, M. Craje, P. Thüne, K.J. Ptasinski, F.J.J.G. Janssen, Olivine as tar removal catalyst for biomass gasifiers: catalyst characterization, Appl. Catal., A Gen. 294 (1) (2005) 68–79.
[45] M. Öhman, A. Nordin, Bed agglomeration characteristics during fluidised bed combustion of biomass fuels, Energy and Fuels 14 (2000) 169–178.
[46] Database Documentation of FACTSage™.